DOI: https://doi.org/10.68732/be3ba85903fd5460

ISBN: 978-9989-2053-6-1

Cyclic thermal treatment of a sandstone from the Upper Rhine Graben

K. M. Neumann, M. Duda & T. Backers
Ruhr University Bochum, Bochum, Germany
Katharina.Neumann-j23@ruhr-uni-bochum.de

Abstract

The share of renewable energy in overall electric energy production is continuously increasing. Renewable energy provision is in parts subject to seasonal and daily fluctuations (solar and wind). In 2025, electricity generation in Germany exceeded consumption on 80+ days. Energy storage concepts are required to minimise this energy loss. Thermal energy storage systems are a key element of an effective storage strategy accelerating the energy transition. Subsurface storage systems in rock mass are particularly interesting because of their abundant availability, and the suitable thermophysical properties of the material.

Changes of the mechanical, thermal, and hydraulic properties upon repeated heating and cooling were investigated to evaluate the impact of the maximum temperature and number of loading cycles on the thermal energy storage medium. A sandstone from the Upper Rhine Graben was selected and heated to maximum temperatures of 200 °C to 600 °C. One cycle comprised heating the specimen to the target temperature in a muffle furnace with a rate of ~ 10 to 11.5 °C/min and cooling to 100 °C with an average rate of ~ 0.5 to 1 °C/min. Further specimens were heated between 100 °C and 200 °C for up to 49 cycles. Before and after thermal treatment density, porosity, P-wave velocity, thermal conductivity, permeability, uniaxial compressive strength and triaxial compressive strength were determined.

Repeated heating to 200 °C in 49 cycles did not cause substantial changes in most rock properties; only the P-wave velocity showed a significant decrease in comparison to one cycle and the reference sample before heating. With increasing maximum temperature, density and P-wave velocity decreased, and effective porosity increased. The most drastic differences were determined for the specimen heated to 600 °C, which can presumably be traced back to the α- to β-quartz transition.

Keywords

Thermal energy storage, Sandstone, Cyclic thermal treatment, Experimental investigation.

1 Introduction

The share of renewable energies in the gross electricity generation of Germany was around 59 % in 2025 (Bundesnetzagentur 2025). The target for 2030 is 80% (Sec. 1 (2) Renewable Energy Act - *Erneuerbare-Energien-Gesetz* 2023). Because of the inherent fluctuations of renewable energy availability, e.g., associated with wind and solar, energy production can exceed energy consumption. In 2025, energy overproduction occurred on 84 days in Germany, corresponding to a total of around 6 Mio. MWh (Bundesnetzagentur 2025). To minimise energy loss, integrating energy storage in power grid planning is a central element. Besides pumped storage plants, thermal energy storage is one of the

most common forms to store energy (Tawalbeh et al. 2023). Subsurface storage in rock mass is particularly interesting, because of its abundance and the suitable thermophysical properties of rock (Tiskatine et al. 2016), as well as its limited above-ground space requirements (Fry et al. 2024). Khatod et al. (2022) conclude that sandstone is an excellent thermal energy storage material because of thehigh specific heat capacity and porosity. However, to evaluate a long-term use of thermal storage systems in siliciclastic rock masses, potential changes in geomechanical and thermal properties of sandstone upon repeated heating and cooling must be evaluated.

Previous studies on various sandstones documented that density, P-wave velocity (Fig. 1a), thermal conductivity and diffusivity decreased with increasing temperature (Hao et al. 2022; Li and Liu 2022; Yang et al. 2017; Sun et al. 2016) and number of cycles (Hou et al. 2020; Zhao et al. 2022). Similarly, Young's modulus and uniaxial compressive strength (UCS) decreased with increasing temperature (Li and Liu 2022; Hou et al. 2020; Fig. 1c and d). Porosity (Hao et al. 2022; Jing et al. 2021; Fig. 1b), permeability (Liu et al. 2020; Yang et al. 2017), and specific heat capacity (Tiskatine et al. 2016) increased with increasing temperature. In contrast to UCS, the triaxial compressive strength in some cases increased with increasing temperature (100 °C to 800 °C, Yang et al. 2017; 25 °C to 950 °C, Li et al. 2022).There are exceptions reported for temperatures up to 200 °C (Li et al. 2022), 300 °C (Hao et al. 2022), or 400 °C (Wang et al. 2023; Vidana and Gratchev 2021; Zhao et al. 2022) where P-wave velocity, Young's modulus and UCS increased slightly or did not change with increasing temperature before ultimately decreasing when the temperature exceeded a particular threshold. For similar temperatures porosity did not change or decreased before increasing at higher temperatures (Hao et al. 2022; Fig. 1b).

UCS and Young's modulus gradually decrease with increasing number of thermal cycles (Vidana and Gratchev 2021; Zhao et al. 2022). A higher number of thermal cycles leads to (slightly) higher porosities according to Becattini et al. (2017) and Vidana and Gratchev (2021). The results from Jing et al. (2021) for temperatures up to 600 °C do not indicate a systematic influence of the number of thermal cycles (1 to 5 cycles) on porosity. Thermal cycles have a significant effect on the rock properties (Vidana and Gratchev 2021) and the influence of the number of cycles on the mechanical properties increases with increasing temperature (Hou et al. 2020).

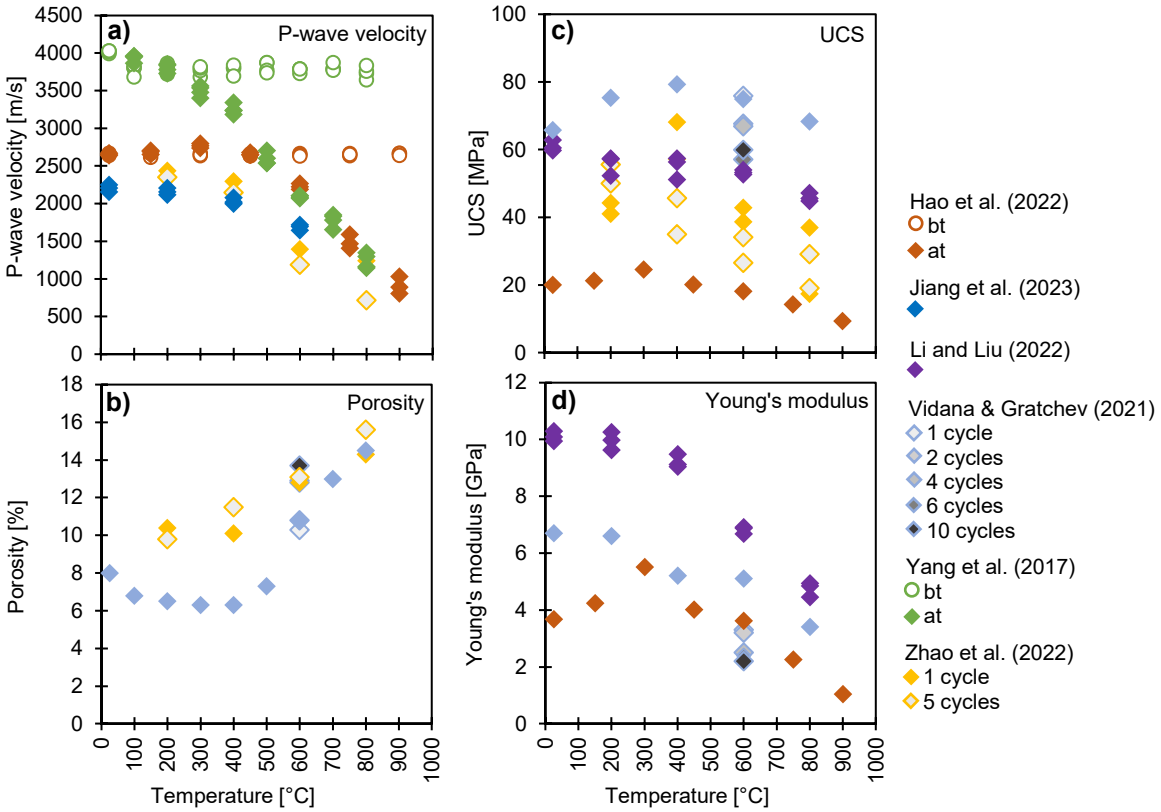


Fig. 1 Comparison of P-wave velocity, UCS, Young's modulus, and porosity after heating sandstone to varying temperatures (and thermal cycles). Sandstone sampling location (mineral composition): Hao et al. (2022) - not specified (21 % qtz., 30 % fsp., 20 % cly., 3 % clc., 16 % o.) , Jiang et al. (2023) - Zigong, China (34 % qtz., 28 % fsp., 28 % cly., 6 % clc., 5 % o.), Li and Liu (2022) - Jiulongpo, China (40 % qtz., 31 % fsp., 14 % cly., 15 % o.), Vidana and Gratchev (2021) - Jimboomba, Australia (39 % qtz., 36 % fsp., 7 % cly., 5 % o.), Yang et al. (2017) - Rizhao, China (mineral composition not specified), Zhao et al. (2022) - Jiangsu, China (qtz., fsp., cly.); Abbreviations: bt - before thermal treatment, at - after thermal treatment, qtz. - quartz, fsp. - feldspar, cly. - clay minerals, clc. - calcite, o. – others.

Due to the high geothermal gradient in the region and the suitable depth and rock properties of the formation, the Buntsandstein (Lower Triassic) in the Upper Rhine Graben (URG) represents a geothermal reservoir of particular interest, which is likely to be increasingly exploited in the future. In this context, potential co-use as thermal energy storage is being examined as part of this study.

2 Material and methods

2.1 Material

A sandstone from a quarry in Neustadt an der Weinstraße, which is located at the western border of the URG between Mannheim and Karlsruhe (Germany), was selected. The rock variety belongs to the Buntsandstein formation (Lower Triassic), has a light beige colour, and contains varying amounts of conglomerates and pores (pore diameters up to ~ 10 mm). The mineralogical composition, determined by X-ray powder diffraction analysis, identified quartz (88 %) and k-feldspar (12 %) as main components, with traces of illite/muscovite and kaolinite (Table 1).

2.2 Methods

Cylindrical cores with a diameter of 42 mm were diamond-drilledperpendicular to beddingand sawed to a length of 84 mm or 21 mm (tensile strength) using water as cooling fluid. The endfaces of the longer cores were ground square to ensure parallelism within 0.02 mm for mechanical testing.Properties of specimens were characterised before and after thermal treatment.

One set of specimens was placed in a muffle furnace and heated to a maximum temperature of 200, 250, 300, 350, 400, 450, 500, 550, or 600 °C with a rate of ~ 10 to 11.5 °C/min, after which the temperature was held for one hour. The specimens were then cooled to 100 °C at an average rate of ~ 0.5 to 1 °C/min, and temperature was again maintained for one hour.

A further set of specimens was heated to an initial temperature of 150 °C (typical in-situ temperature of the Buntsandstein in the URG) with a rate of around 4 to 5 °C/min, which was held for one hour. The specimens were then heated with ~ 2.5 °C/min to a maximum temperature of 200 °C. After holding this temperature for one hour, the specimens were cooled to 100 °C with a rate of ~ 0.5 °C/min, which was again maintained for one hour. For specimens subjected to repeated thermal cycles, the temperature was again raised to 200 °C with about 7 °C/min. Thermal cycles from 100 °C to 200 °C were then repeated up to 49 times. To account for specimen variability, three specimens were tested for each maximum temperature or number of cycles.

Bulk density of oven-dried rock specimens was derived from the ratio of mass and volume. Grain density was determined by milling a representative sample of the sandstone to powder, which was then analysed by pycnometry using distilled water (DIN EN ISO 17892-3).Total porosity of specimens was calculated from the ratio of their bulk density to grain density, and effective porosity was determined from water uptake. P-wave velocity was determined with a standard measurement device (Geotron Elektronik) with two identical P-wave ultrasound sensors in axial and two radial directions with a signal frequency of about 350 kHz emitted from the waveform generator. No coupling medium was used between the sensors and the specimen.

Thermal conductivity and effusivity were determined with a Modified Transient Plane Source (MTPS) sensor using C-Therm's Trident system on cylindrical samples (Harris et al. 2014). A short current pulse is applied to the sensor's spiral heating element, which causes a temperature increase by 1 to 3 °C as the heat diffuses into the specimen in one-dimensional heat flow (ASTM D7984-16). A thermal joint compound (type 120 silicone from Wakefield Thermal) was used as a coupling agent and a 500 g weight was placed on top of the specimens to standardise coupling. Heat capacity was derived from thermal conductivity, effusivity and bulk density of the specimens. Thermal diffusivity was calculated from thermal conductivity, heat capacity and bulk density of the specimens.

UCS, tensile strength (TS) and triaxial compressive strength (TCS) were determined using a stiff 4000 kN loading frame. For UCS, specimens were centered between loading plates and axially loaded ata strain rate of about 10^{-5} s^{-1}. Axial stresses and strains were calculated based on the cross-sectional area and sample length of the specimen before testing. Axial strains were calibrated for system stiffness. UCS was derived from the maximum in the stress-strain-relation. Young's modulus was determined between 40 % and 60 % of UCS. For TS, specimen discs were placed in a steel loading jaw and loaded at a rate of 2.5 µm/s until failure (ISRM 1978). Multi-stage triaxial compressive strength tests were performed using a Hoek cell at confining pressures of 20 MPa, 15 MPa, and 10 MPa. For each pressure stage, the maximum axial stress at failure was determined (ISRM 1978).

3 Results

3.1 Temperature

Specimens that were heated to a maximum temperature of ≥300 °C developed a reddish colour. Yet, mineralogy did not change systematically considering uncertainties of ± 2-5 % (Table 1) and specimen variability. Density decreased by up to 0.8 % with increasing maximum temperature (Fig. 2a), while effective porosity increased by about 4 % (Fig. 2b) compared to before thermal treatment. A significant change in density was observed for specimens heated to ≥350 °C. Effective porosity increased significantly for maximum temperatures of ≥450 °C. P-wave velocities show the most significant change from the untreated state. With increasing maximum temperature, axial and radial P-wave velocities decreased with a maximum decrease of around 45 % for 600 °C (Fig. 2c and d). These results could be reproduced for specimens drilled parallel to bedding. For UCS no systematic relation to maximum temperature can be observed (Fig. 2e), results mainly vary within the range of specimen variability. Young's modulus shows a slightly decreasing trend with increasing temperature (Fig. 2f).

Table 1. XRD-analysis results in volume-% (converting mass-% to volume-% may result in deviations from 100% in the sum of the rounded values), uncertainty +/- 2-5 %, bt - before thermal treatment.

mineral	**bt**	**200 °C 49 cycles**	**300 °C 1 cycle**	**400 °C 1 cycle**	**500 °C 1 cycle**	**600 °C 1 cycle**
quartz	88	87	86	85	85	89
orthoclase	12	11	11	12	13	10
illite/muscovite	traces	2	2	2	2	2
kaolinite	traces		1	1	traces	0

3.2 Cycles

Heating the sandstone specimens to 1 or 49 cycles did not significantly affect colour or mineralogical composition (Table 1), density, porosity, thermal conductivity, Young's modulus, or TS. UCS and TCS also did not show systematic changes when comparing heated to untreated specimens (

Fig. 3a). P-wave velocity, however, decreased significantly

Fig. 3b). A thin section of a heated specimen showed some presumably thermally induced cracks after heating to 200 °C in 49 cycles. Compared to the thin section of an untreated specimen, the number of cracks appears to increase with thermal treatment. A quantitative analysis is pending for future investigations.

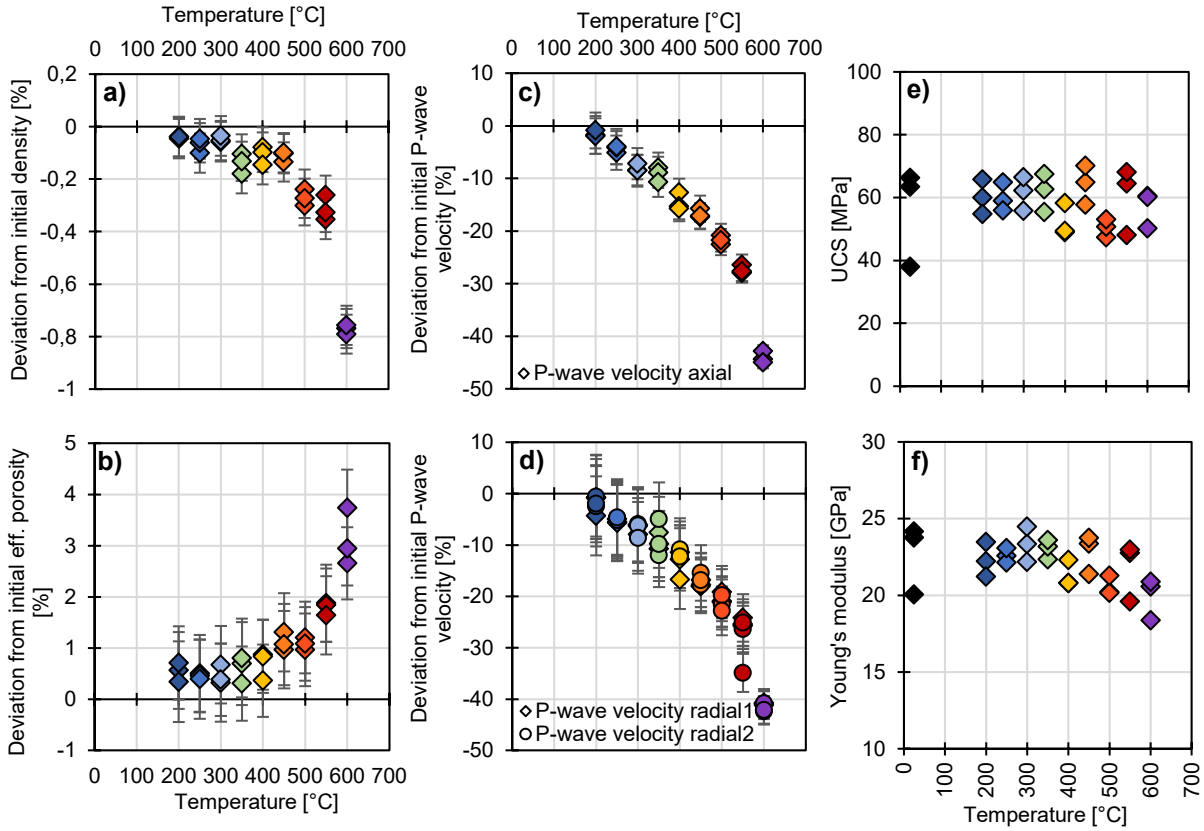


Fig. 2 Results for specimen heated up to 600 °C for 1 thermal cycle, percentage deviation of the results after heating the samples compared to before heating; eff. porosity - effective porosity, P-wave velocity axial/radial - measured in axial/radial direction of the specimen; colours to differentiate temperatures.

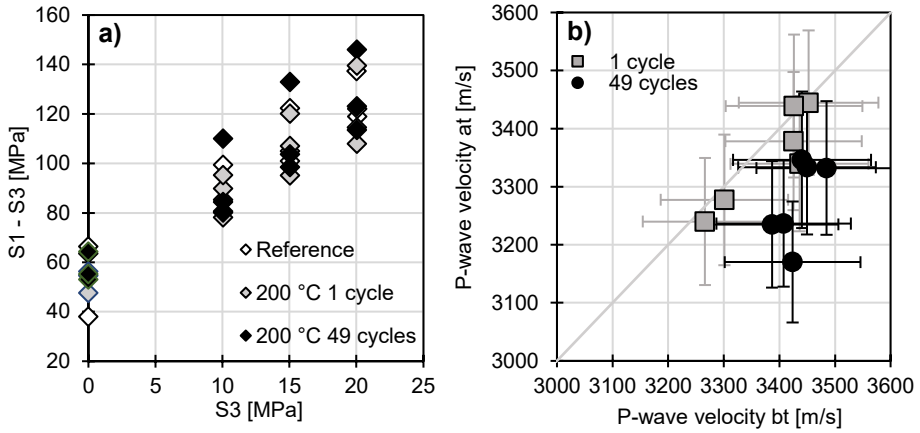


Fig. 3 a) Results from UCS and triaxial compressive strength tests for untreated samples (white), samples heated to max. 200 °C for 1 cycle (grey), and 49 cycles (black), b) P-wave velocity measured in axial direction before thermal treatment (bt, x-axis) and after thermal treatment (at, y-axis) for samples heated to max. 200 °C for 1 cycle (grey) and 49 cycles (black).

4 Discussion

The change of colour, density, porosity, and P-wave velocity of heated specimens compared to their untreated references are consistent with observations reported in other studies (e.g., Hao et al. 2022; Jing et al. 2021; Li and Liu 2022; Vidana and Gratchev 2021; Yang et al. 2017; Zhao et al. 2022). A pronounced increase in porosity after heating sandstone to a maximum of 400 °C can also be found in several other studies (Hao et al. 2022; Jing et al. 2021; Li and Liu 2022; Liu et al. 2020; Vidana and Gratchev 2021; Sun et al. 2016; Zhao et al. 2022). The observed decrease in P-wave velocity with increasing number of cycles was previously reported by Hou et al. (2020), and Zhao et al. (2022). Thermal expansion of the minerals and associated formation of microcracks may explain this observation; thin section analysis supports this interpretation. XRD analyses show no changes beyond analytical uncertainties for heated samples compared to untreated samples (Table 1), but the colour change suggests thermal alterations. Young's modulus shows a decreasing trend comparable to the results of Hao et al. (2022), with a peak at 300 °C (c.f. Fig. 1d &Fig. 2f), which is consistent with the

decreasing P-wave velocity, as a lower P-wave velocity corresponds to a lower Young's modulus. However, contrary to e.g. Li and Liu (2022), Hao et al. (2022) or Hou et al. (2020), the changes in Young's modulus are minor and not related to UCS considering specimen variability. Increasing the number of cycles from 1 to 49 at 200 °C did not result in changes in UCS, Young's modulus (as in Vidana and Gratchev 2021, or Zhao et al. 2022), or triaxial compressive strength, but in P-wave velocity (consistent with Hou et al. 2020, and Zhao et al. 2022; c.f.

Fig. 3b).

5 Conclusion

Repeated heating and cooling of sandstone up to 49 times to a maximum temperature of 200 °C leads to irreversible microstructural changes, resulting in reduced P-wave velocities. Increasing the maximum temperature to 600 °C amplifies the impact on the rock's properties such as density, effective porosity, and P-wave velocity. The potential to induce irreversible changes in the rock mass must be accounted for (e.g. adjusting injection temperatures, depths, etc.), when considering a sandstone reservoir for thermal energy storage.

Aspects of this work have been performed within the projects AGENS (funded by the German Federal Ministry for Economic Affairs and Energy), and LISAGENS (funded by the German Federal Ministry of Research, Technology, and Space). We acknowledge the support for our research.

References

ASTM D7984-16 (2016) Standard test method for measurement of thermal effusivity of fabrics using a modified transient plane source (mtps) instrument

Becattini V, Motmans T, ZapponeA, Madonna C, Haselbacher A, Steinfeld A (2017) Experimental investigation of the thermal and mechanical stability of rocks for high-temperature thermal-energy storage. AppliedEnergy203: 373–389.https://doi.org/10.1016/j.apenergy.2017.06.025.

Bundesnetzagentur (2026) SMARD - Strom- und Gasmarktdaten.https://www.smard.de. Accessed at 11.02.2026

DIN EN ISO 17892-3 (2015) Geotechnische Erkundung und Untersuchung - Laborversuche an Bodenproben - Teil 3: Bestimmung der Korndichte

Erneuerbare-Energien-Gesetz - EEG (2023)

Fry N, Adebayo P, Tian R, Shor R, Mwesigye A (2024) A review of district energy technology with subsurface thermal storage integration. GeothermalEnergy12(1): 29. https://doi.org/10.1186/s40517-024-00308-3.

Hao J, Qiao L, Liu Z, Li Q (2022) Effect of thermal treatment on physical and mechanical properties of sandstone for thermal energy storage: a comprehensive experimental study. ActaGeotechnica,17(9): 3887-3908. https://doi.org/10.1007/s11440-022-01514-8.

Harris A, Kazachenko S, Bateman R, Nickerson J, Emanuel M (2014) Measuring the thermal conductivity of heat transfer fluids via the modified transient plane source (mtps) JournalofThermalAnalysisandCalorimetry116: 1309-1314.

Hou P, Gao L, Xing Y, ZhangZP (2020). Effect of thermal cycling on mechanical properties and energy evolution of sandstone. ThermalScience24(6 Part B): 4001-4009. https://doi.org/10.2298/TSCI2006001H.

ISRM (1978) Suggested methods for determining tensile strength of rock materials part 2: suggested method for determining indirect tensile strength by the brazil test. InternationalJournalofRockMechanicsandMiningSciences15 (3): 99–103

ISRM (1978) Suggested methods for determining the strength of rock materials in triaxial compression. InternationalJournalofRockMechanicsandMiningSciences15 (2): 47-51

ISRM (1979) Suggested methods for determining the uniaxial compressive strength and deformability of rock materials: part 1. suggested method for determining deformability of rock materials in uniaxial compression. InternationalJournalofRockMechanicsandMiningSciences16 (2): 138-140.

Jiang Y, Su H, Zhang L, Yu L, Chen G (2023). Heating-path dependency of fracture behavior of sandstone subjected to thermal treatment. TheoreticalandAppliedFractureMechanics127 104096. https://doi.org/10.1016/j.tafmec.2023.104096.

Jing X, Sun Q, Jia H, Ge Z, Wang T (2021). Influence of high-temperature thermal cycles on the pore structure of red sandstone. BulletinofEngineeringGeologyandtheEnvironment80(10): 7817-7830. https://doi.org/10.1007/s10064-021-02389-x.

Khatod KJ, Katekar VP, Deshmukh SS (2022) An evaluation for the optimal sensible heat storage material for maximizing solar still productivity: A state-of-the-art review. JournalofEnergyStorage50 (104622). https://doi.org/10.1016/j.est.2022.104622.

Li M, and Liu X (2022) Effect of Thermal Treatment on the Physical and Mechanical Properties of Sandstone: Insights from Experiments and Simulations. RockMechanicsandRockEngineering55(6): 3171-3194. https://doi.org/10.1007/s00603-022-02791-1.

Li X, Peng J, Xie Y, Li Q, Zhou T, Wang J, Zheng W (2022) Influence of High-Temperature Treatment on Strength and Failure Behaviors of a Quartz-Rich Sandstone under True Triaxial Condition. Lithosphere2022(Special 10). https://doi.org/10.2113/2022/3086647.

Liu X, Lu W, Li M, Zeng N, Li T (2020) The Thermal Effect on the Physical Properties and Corresponding Permeability Evolution of the Heat-Treated Sandstones. Geofluids 2020: 1-16. https://doi.org/10.1155/2020/8838325.

Sun Q, Lü C, Cao L, Li W, Geng J, Zhang W (2016) Thermal Properties of Sandstone After Treatment at High Temperature. InternationalJournalofRockMechanicsandMiningSciences85: 60-66. https://doi.org/10.1016/j.ijrmms.2016.03.006.

Tawalbeh M, Khan HA, Al-Othman A, Almomani F, Ajith S (2023) A comprehensive review on the recent advances in materials for thermal energy storage applications. InternationalJournalofThermofluids18 (100326). https://doi.org/10.1016/j.ijft.2023.100326.

Tiskatine R, Bougdour N, Idoum A, Bazgaou A, Oaddi R, Ihlal A, Aharoune A (2023) Experimental investigation on rock thermal properties under the influence of temperature. Thermochimica Acta720 179424. https://doi.org/10.1016/j.tca.2022.179424

Vidana Pathiranagei S, and Gratchev I (2021) Engineering properties of sandstone heated to a range of high temperatures. BulletinofEngineeringGeologyandtheEnvironment80(3): 2415-2432. https://doi.org/10.1007/s10064-020-02065-6.

Wang M, Li J, Tan H, Wang J, Shi Z, Li K (2023) Study on fatigue characteristics and thermal damage mechanism of red sandstone under high temperature-cyclic load coupling. InternationalJournalofFatigue,168 (107405). https://doi.org/10.1016/j.ijfatigue.2022.107405.

Yang SQ, Xu P, Li YB, Huang YH (2017) Experimental investigation on triaxial mechanical and permeability behavior of sandstone after exposure to different high temperature treatments. Geothermics69: 93-109. https://doi.org/10.1016/j.geothermics.2017.04.009.

Zhao Y, Du C, Bi J, Li J, Wang C (2022) Influence of multiple porous structure evolution on physical–mechanical properties and damage mechanism of sandstone heated continuously/periodically with the identical heating time. BulletinofEngineeringGeologyandtheEnvironment81(12): 507. https://doi.org/10.1007/s10064-022-03020-3.